Experimental performance evaluation of quadrature amplitude modulation signal transmission in a silicon microring

Chengcheng Gui and Jian Wang*

Wuhan National Laboratory for Optoelectronics, School of Optical and Electronic Information, Huazhong University of Science and Technology, Wuhan 430074, Hubei, China
**Corresponding author: jwang@hust.edu.cn*

Received May 18, 2016; revised July 15, 2016; accepted July 20, 2016;
posted July 22, 2016 (Doc. ID 266576); published September 1, 2016

We comprehensively characterize the transmission performance of m-ary quadrature amplitude modulation (m-QAM) signals through a silicon microring resonator in the experiment. Using orthogonal frequency-division multiplexing based on offset QAM (OFDM/OQAM) which is modulated with m-QAM modulations, we demonstrate low-penalty data transmission of OFDM/OQAM 64-QAM, 128-QAM, 256-QAM, and 512-QAM signals in a silicon microring resonator. The observed optical signal-to-noise ratio (OSNR) penalties are 1.7 dB for 64-QAM, 1.7 dB for 128-QAM, and 3.1 dB for 256-QAM at a bit-error rate (BER) of 2×10^{-3} and 3.3 dB for 512-QAM at a BER of 2×10^{-2}. The performance degradation due to the wavelength detuning from the microring resonance is evaluated, showing a wavelength range of ~0.48 nm with BER below 2×10^{-3}. Moreover, we demonstrate data transmission of 191.2-Gbit/s simultaneous eight wavelength channel OFDM/OQAM 256-QAM signals in a silicon microring resonator, achieving OSNR penalties less than 2 dB at a BER of 2×10^{-2}.

OCIS codes: (130.3120) Integrated optics devices; (220.0220) Optical design and fabrication; (230.7370) Waveguides; (060.4510) Optical communications.
http://dx.doi.org/10.1364/PRJ.4.000168

1. INTRODUCTION

The rapid growth of Internet, high-speed data, and multimedia services has given rise to ever increasing demand for high data traffic rates and transmission capacity. Compared to electronic integrated circuits, photonic integrated circuits (PICs) feature higher data transmission rates [1]. Recently, PICs, which have facilitated possible integration of complete optical communication systems on a monolithic semiconductor chip, are envisioned as promising ways of implementing on-chip and chip-to-chip interconnection networks [2–4]. PIC-assisted optical interconnection provides relaxed interconnection latency, wide bandwidth, and high resistance to electromagnetic interference. Several optical technologies have been developed including the use of silicon photonics [5,6], photonic crystals [7], and plasmonic circuits [8]. Remarkably, owing to the availability of a mature silicon technology, lower power consumption, compactness, and potential for complementary metal-oxide-semiconductor compatibility, silicon photonics is considered to be a promising technology to address the ever increasing challenges of future chip-scale optical interconnections and optical data processing [9–13]. Among the many researched silicon photonic devices, microring resonators feature a compact structure capable of performing a variety of network functions (i.e., wavelength conversion, optical switching, optical filters, optical delay lines, microwave photonic filters) [14–20]. Because of the unprecedented bandwidth scalability with reduced power consumption enabled by high-performance silicon photonic devices, the wavelength-division multiplexing (WDM) technique can be employed to achieve high data rates and make wavelength parallelism available in integrated optics [21,22]. So far ultrahigh-speed data transmission of Tbit/s signals has been reported in optical fiber transmission systems [23]. In this scenario, one expected challenge would be high-speed data transmission for on-chip networks. In the past few years, data transmissions of multichannel 40-Gbit/s binary on–off keying (OOK) signals in a silicon waveguide [24], 170-Gbit/s OOK signals in an erbium-doped waveguide amplifier on silicon [25], and 40-Gbit/s binary differential phase-shift keying (DPSK) transmission through a silicon microring switch [15] have been reported, showing impressive performance. With unabated exponential growth of data traffic, advanced multilevel modulation formats such as m-ary phase-shift keying (m-PSK) and m-ary quadrature amplitude modulation (m-QAM), and multiplexing techniques such as WDM and orthogonal frequency-division multiplexing (OFDM), have become of great importance to increase the capacity and spectral efficiency of communication systems [23,26]. Hence, one laudable goal would be to realize high-speed optical data transmission of m-QAM signals in silicon photonic devices. Very recently, terabit-scale data transmission of WDM OFDM 16-QAM signals through silicon vertical slot waveguides has been reported [27]. Additionally, owing to the high side lobe suppression ratio, OFDM based on offset QAM (OFDM/OQAM), which can be modulated with high order PSK or QAM modulations, has recently attracted increasing attention in optical communications [28,29]. However, optical data transmission of OFDM/OQAM m-QAM signals in silicon photonic devices (e.g., silicon microring resonators) has not yet been reported.

In this paper, we experimentally study the transmission performance of OFDM/OQAM m-QAM signals through a silicon microring resonator. Low-penalty transmissions of OFDM/OQAM 64-QAM, 128-QAM, 256-QAM, and 512-QAM signals in a silicon microring resonator are demonstrated. The transmission impairments induced by the wavelength detuning from the microring resonance are discussed. Meanwhile, the transmission performance of 191.2-Gbit/s simultaneous eight-channel WDM OFDM/OQAM 256-QAM signals in a silicon microring resonator is also evaluated.

2. EXPERIMENTAL SETUP AND SILICON PHOTONIC DEVICE

The experimental setup for data transmission of OFDM/OQAM m-QAM signals through a silicon microring resonator is shown in Fig. 1. At the transmitter side, the outputs of eight external cavity lasers (ECLs) are injected into eight polarization controllers (PCs) and then combined by wavelength selective switches (WSSs) and an optical coupler (OC). The eight laser wavelengths are set to be 1544.54, 1546.41, 1548.28, 1550.15, 1552.02, 1553.89, 1555.76, and 1557.63 nm. The combined eight wavelength channels pass through an optical inphase/quadrature (IQ) modulator to carry OFDM/OQAM m-QAM signals. An arbitrary waveform generator (AWG) running at 10 Gsamples/s is employed to produce single sideband electrical signal. The effective numbers of bits of the AWG and scope are 10 and 10, respectively, and the sampling rates of the AWG and scope are 10 and 50 Gsamples/s, respectively. The OFDM/OQAM signal is constructed by 82 subcarriers, in which 78 subcarriers are loaded with payloads using m-QAM ($m \geq 64$) modulation mapping, while 4 subcarriers are selected as the pilots with 4-QAM loading to estimate the phase noise. For the purpose of channel estimation, we employ 10 training symbols for every 500 payload symbols. Only one polarization is used for the transmission. The symbol rate is 3 Gbaud ($10 \times 78/256 = 3$ Gbaud). The OFDM/OQAM m-QAM signals are amplified by an erbium-doped fiber amplifier (EDFA) and then coupled to a silicon photonic device by a vertical grating coupler.

The silicon photonic device is fabricated on a silicon-on-insulator wafer with a 340-nm-thick top silicon layer and a 2-μm-thick buried oxide layer. The device layout is transferred to ZEP520A photoresist by electron-beam lithography (EBL; Vistec EBPG5000 + ES). Using EBL followed by induced coupled plasma etching (Oxford Instruments Plasmalab System 100), the proposed silicon photonic device structure is formed by the upper silicon layer, which is etched downward to 220 nm. Our silicon device is composed of a bus waveguide and a microring. Vertical grating couplers are used to couple light in and out of the bus waveguide, and they prohibit transmitting TM mode and ensure operation with TE-polarized light only. So the single mode (TE mode) transmits in the proposed silicon photonic device. To improve fiber-to-waveguide coupling efficiency, a nominal 1200-nm-wide waveguide is linearly tapered to 500 nm between the nanowire and vertical grating coupler. The scanning electron microscope (SEM) image of the bus waveguide with dimensions of 500 nm wide × 220 nm thick is shown in Fig. 1(a). Figure 1(b) depicts the SEM image of the microring structure. The radius and height are 50 μm and 220 nm, respectively. The zoomed-in coupling region is depicted in Fig. 1(c). The coupling gap between the bus waveguide and bending waveguide of the microring is about 240 nm. Figure 1(d) exhibits the zoomed-in vertical grating coupler. The period of the vertical grating coupler is 630 nm, and the duty cycle is 50%. The coupling loss of the vertical grating coupler is measured to be 7 dB for a single side.

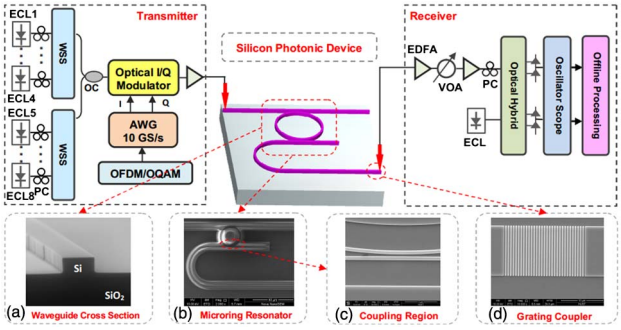

Fig. 1. Experimental setup for data transmission of OFDM/OQAM m-QAM signals through a silicon microring resonator. (a)-(d) SEM images of (a) waveguide cross section, (b) mirroring resonator, (c) coupling region between the bus waveguide and bending waveguide, and (d) grating coupler.

The signal transmitting through the silicon photonic device is coupled out by another vertical grating coupler and then amplified by an EDFA. A variable optical attenuator (VOA) is employed to adjust the optical signal-to-noise ratio (OSNR). At the receiver side, a local oscillator is used to mix the received signal in a coherent receiver. For on-chip single polarization transmission, a PC is employed to align the polarization states. The radio-frequency (RF) signals corresponding to I/Q components are fed into a Tektronix real-time scope and processed offline with a MATLAB program. The offline digital signal processing contains (1) carrier frequency offset estimation and OFDM window synchronization, (2) digital filter designed for OFDM/OQAM only, (3) fast Fourier transform (FFT), (4) channel estimation and phase noise estimation, and (5) constellation decision and bit-error rate (BER) calculation. A synchronization sequence is used at the front end of the frame data to estimate carrier frequency offset and synchronize the OFDM window. After FFT, the signal is converted to the frequency domain. For the channel estimation, we employ 10 training symbols for every 468 payload symbols in a manner of [A 0], where "A" denotes one OFDM m-QAM symbol.

3. EXPERIMENTAL RESULTS AND DISCUSSION

First, we experimentally study the data transmission performance through the silicon photonic device using OFDM/OQAM m-QAM signals. In the experiment, we select the fourth wavelength channel (i.e., 1550.15 nm), loading it with OFDM/OQAM 64-QAM, 128-QAM, 256-QAM, and 512-QAM modulations for the data transmission through a microring resonator. The corresponding net data rates for each format are 17.9, 20.9, 23.9, and 26.9 Gbit/s, respectively. Figure 2(a) shows the measured transmission spectrum of the fabricated microring resonator with an observed free spectral range of ~1.87 nm using an optical spectrum analyzer (AQ6370B). The bandwidth resolution of the spectrum measurements we used is 0.02 nm. The zoomed-in spectrum in Fig. 2(b)

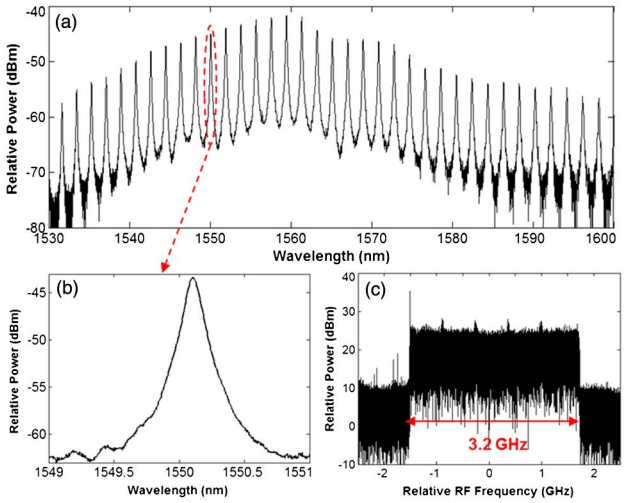

Fig. 2. (a) Measured transmission spectrum of fabricated microring resonator. (b) Zoomed-in spectrum of selected resonance in the experiment. (c) RF spectrum of demodulated signal.

shows the selected resonance wavelength (~1550.15 nm) of the fabricated microring resonator in the experiment with an extinction ratio of ~19.4 dB. Figure 2(c) plots the measured RF spectrum of the demodulated signal at the offline digital signal processor with a bandwidth of 3.2 GHz.

The measured BER curves for OFDM/OQAM m-QAM data transmission as a function of the received OSNR are plotted in Figs. 3(a)–3(d). The observed OSNR penalty is assessed to be 1.7, 1.7, and 3.1 dB at a BER of 2×10^{-3} (enhanced forward error correction [EFEC] threshold) for OFDM/OQAM 64-QAM, 128-QAM, and 256-QAM, respectively. For the data transmission of OFDM/OQAM 512-QAM, the OSNR penalty is measured to be less than 3.3 dB at a BER of 2×10^{-2} (20% overhead forward error correction [FEC] threshold). The measured constellations of transmitted m-QAM ($m \geq 64$)

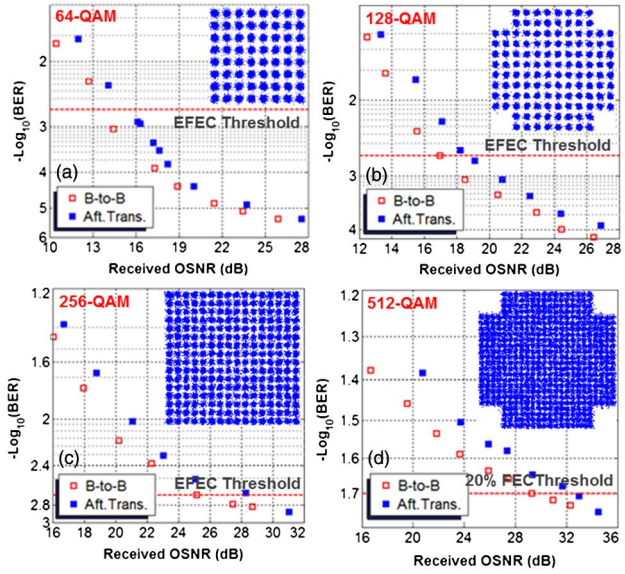

Fig. 3. BER versus received OSNR for data transmission of OFDM/OQAM m-QAM signal through a silicon microring resonator. (a) 64-QAM. (b) 128-QAM. (c) 256-QAM. (d) 512-QAM. Inserts are constellations of signal after transmission. B-to-B, back-to-back; Aft. Trans., after transmission.

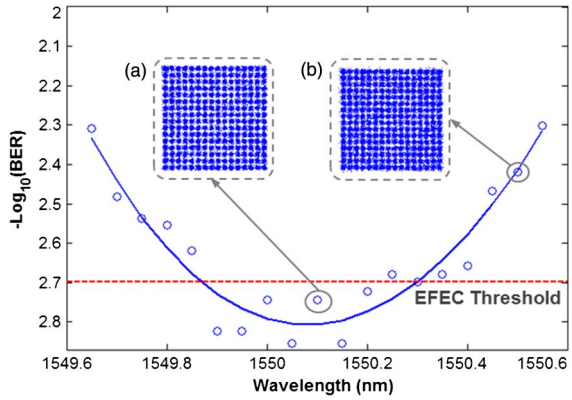

Fig. 4. BER versus signal wavelength detuning from the microring resonance wavelength for experimental measurements (circles) and fitting curve (solid line). Insets are constellations of 256-QAM signals.

signals through the proposed silicon photonic device are depicted in the insets of Fig. 3.

Then, we shift the wavelength of the transmitted OFDM/OQAM 256-QAM signal to evaluate the performance degradation due to the wavelength detuning from the microring resonance wavelength. Figure 4 shows measured BER performance as a function of the signal wavelength detuning from the microring resonance wavelength. One can see that the measured BER values can be kept below the EFEC threshold of 2×10^{-3} as the signal wavelength is varied from 1549.84 to 1550.32 nm, that is, within a wavelength range of ~0.48 nm. When the signal wavelength is further detuned from the microring resonance, significant performance degradation is observed. As shown in Fig. 4, a fitting curve is also plotted for reference. The insets (a) and (b) in Fig. 4 depict two examples of measured constellations which clearly show the performance degradation due to the relatively large signal wavelength detuning from the microring resonance wavelength. Such wavelength detuning-induced performance degradation

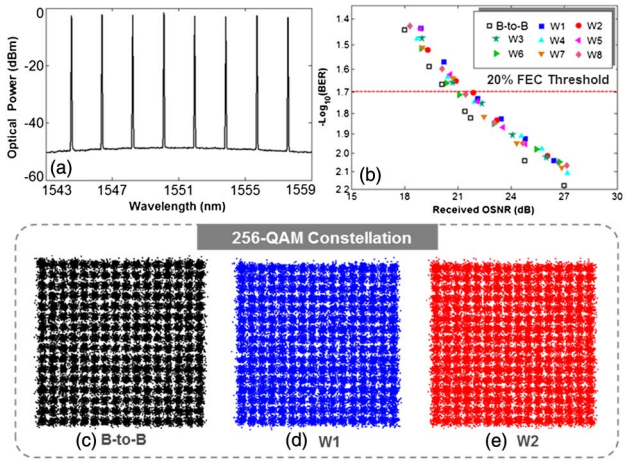

Fig. 5. (a) Input spectrum of eight wavelength channels before the input of the modulator. (b) BER versus received OSNR for all eight-channel OFDM/OQAM 256-QAM data transmission. (c)–(e) Constellations of (c) B-to-B signal at 1554.54 nm, transmitted signals at (d) 1544.54 and (e) 1546.41 nm. B-to-B, back-to-back; W1, 1544.54 nm; W2, 1546.41 nm; W3, 1548.28 nm; W4, 1550.15 nm; W5, 1552.02 nm; W6, 1553.89 nm; W7, 1555.76 nm; W8, 1557.63 nm.

can be ascribed to the filtering impairments when transmitting the signal through the passband of microring resonator.

Additionally, we study the wavelength parallelism by transmitting 191.2-Gbit/s simultaneous eight-channel WDM OFDM/OQAM 256-QAM signals through the fabricated microring resonator. The eight laser wavelengths are set to be 1544.54, 1546.41, 1548.28, 1550.15, 1552.02, 1553.89, 1555.76, and 1557.63 nm, respectively. The combined eight wavelength channels are combined by the OC and then pass through an optical IQ modulator to carry OFDM/OQAM m-QAM signals. Figure 5(a) shows the observed input spectrum of the eight wavelength channels before being modulated by the optical IQ modulator. The measured BER curves for all eight-channel OFDM/OQAM 256-QAM data transmission as a function of the received OSNR are shown in Fig. 5(b). The observed OSNR penalties are less than 2 dB at a BER of 2×10^{-2} (20% FEC threshold). Figures 5(c)–5(e) display three examples of measured constellations of back-to-back (B-to-B) OFDM/OQAM 256-QAM signal at 1554.54 nm and transmitted OFDM/OQAM 256-QAM signals at 1544.54 and 1546.41 nm, respectively.

4. CONCLUSIONS

In summary, the obtained results shown in Figs. 3–5 indicate the successful low-penalty transmission of OFDM/OQAM m-QAM signals through a silicon microring resonator. OFDM/OQAM 64-QAM, 128-QAM, 256-QAM, and 512-QAM data transmissions are demonstrated in the experiment. The impairments from the signal wavelength detuning from the microring resonance are discussed. Moreover, simultaneous eight-channel WDM OFDM/OQAM 256-QAM data transmission through the microring resonator is implemented. With further improvement, the fabricated silicon microring resonator might support simultaneous WDM m-QAM data transmission with even more wavelength channels (>8).

Funding. National Program for Support of Top-Notch Young Professionals; National Natural Science Foundation of China (NSFC) (11574001, 11274131, 61222502); Program for New Century Excellent Talents in University (NCET) (NCET-11-0182).

Acknowledgment. The authors thank Qingzhong Huang, Jinsong Xia, and Xiaoping Li in the Center of Micro-Fabrication and Characterization of Wuhan National Laboratory for Optoelectronics (WNLO) for the support in the manufacturing process of silicon microring resonators. The authors also thank the facility support of the Center for Nanoscale Characterization and Devices of WNLO. The authors would like to thank Chao Li and Qi Yang for their technical support and helpful discussions.

REFERENCES

1. D. A. B. Miller, "Rationale and challenges for optical interconnects to electronic chips," Proc. IEEE **88**, 728–749 (2000).
2. M. J. Kobrinsky, B. A. Block, J.-F. Zheng, B. C. Barnett, E. Mohammed, M. Reshotko, F. Robertson, S. List, I. Young, and K. Cadien, "On-chip optical interconnects," Int. Technol. J. **8**, 129–141 (2004).
3. A. Shacham, K. Bergman, and L. P. Carloni, "Photonic networks-on-chip for future generations of chip multiprocessors," IEEE. Trans. Comput. **57**, 1246–1260 (2008).
4. J. D. Owens, W. J. Dally, R. Ho, D. J. Jayasimha, S. W. Keckler, and L.-S. Peh, "Research challenges for on-chip interconnection networks," IEEE Micro **27**, 96–108 (2007).
5. F. Xia, M. J. Rooks, L. Sekaric, and Y. A. Vlasov, "Ultra-compact high order ring resonator filters using submicron silicon photonic wires for on-chip optical interconnects," Opt. Express **15**, 11934–11941 (2007).
6. Y. Vlasov, W. M. J. Green, and F. Xia, "High-throughput silicon nanophotonic wavelength-insensitive switch for on-chip optical networks," Nat. Photonics **2**, 242–246 (2008).
7. S. J. Mcnab, N. Moll, and Y. A. Vlasov, "Ultra-low loss photonic integrated circuit with membrane-type photonic crystal waveguides," Opt. Express **11**, 2927–2939 (2003).
8. J. T. Kim, J. J. Ju, S. Park, M. Kim, S. K. Park, and M.-H. Lee, "Chip-to-chip optical interconnect using gold long-range surface plasmon polarition waveguides," Opt. Express **16**, 13133–13138 (2008).
9. R. Soref, "The past, present, and future of silicon photonics," IEEE J. Sel. Top. Quantum Electron. **12**, 1678–1687 (2006).
10. B. Jalali and S. Fathpour, "Silicon photonics," J. Lightwave Technol. **24**, 4600–4615 (2007).
11. M. Asghari and A. V. Krishnamoorthy, "Silicon photonics: energy-efficient communication," Nat. Photonics **5**, 268–270 (2011).
12. Y. Long, A. Wang, L. Zhou, and J. Wang, "All-optical wavelength conversion and signal regeneration of PAM-4 signal using a silicon waveguide," Opt. Express **24**, 7158–7167 (2016).
13. L. K. Oxenlowe, H. Ji, M. Galili, and M. Pu, "Silicon photonics for signal processing of Tbit/s serial data signals," IEEE J. Sel. Top. Quantum Electron. **18**, 996–1005 (2012).
14. X. Hu, Y. Long, M. Ji, A. Wang, L. Zhu, Z. Ruan, Y. Wang, and J. Wang, "Graphene–silicon microring resonator enhanced all-optical up and down wavelength conversion of QPSK signal," Opt. Express **24**, 7168–7177 (2016).
15. L. Xu, W. Zhang, Q. Li, J. Chan, H. L. R. Lira, M. Lipson, and K. Bergman, "40-Gb/s DPSK data transmission through a silicon microring switch," IEEE Photon. Technol. Lett. **24**, 473–475 (2012).
16. Y. Long and J. Wang, "Optically-controlled extinction ratio and *Q*-factor tunable silicon microring resonators based on optical forces," Sci. Rep. **4**, 5409 (2014).
17. H. L. Lira, C. B. Poitras, and M. Lipson, "CMOS compatible reconfigurable filter for high bandwidth non-blocking operation," Opt. Express **19**, 20115–20121 (2011).
18. J. Cardenas, M. A. Foster, N. Sherwood-Droz, C. B. Poitras, H. L. R. Lira, B. Zhang, A. L. Gaeta, J. B. Khurgin, P. Morton, and M. Lipson, "Wide-bandwidth continuously tunable optical delay line using silicon microring resonators," Opt. Express **18**, 26525–26534 (2010).
19. Y. Long and J. Wang, "Ultra-high peak rejection notch microwave photonic filter using a single silicon microring resonator," Opt. Express **23**, 17739–17750 (2015).
20. Y. Long and J. Wang, "All-optical tuning of a nonlinear silicon microring assisted microwave photonic filter: theory and experiment," Opt. Express **23**, 17758–17771 (2015).
21. X. Chen, B. G. Lee, X. Liu, B. A. Small, I. Hsieh, J. Dadap, K. Bergman, and R. M. Osgood, Jr., "Demonstration of 300 Gbps error-free transmission of WDM data stream in silicon photonic wires," in *Proceedings of Conference on Lasers Electro-Optics (CLEO)*, Baltimore, Maryland, (2007), paper CtuQ5.
22. Y. Long, J. Liu, X. Hu, A. Wang, L. Zhou, K. Zou, Y. Zhu, F. Zhang, and J. Wang, "All-optical multi-channel wavelength conversion of Nyquist 16-QAM signal using a silicon waveguide," Opt. Lett. **40**, 5475–5478 (2015).
23. D. Qian, M.-F. Huang, E. Ip, Y.-K. Huang, Y. Shao, J. Hu, and T. Wang, "High capacity/spectral efficiency 101.7-Tb/s WDM transmission using PDM-128QAM-OFDM over 165-km SSMF within C- and L-bands," J. Lightwave Technol. **30**, 1540–1548 (2012).
24. B. G. Lee, X. Chen, A. Biberman, X. Liu, I.-W. Hsieh, C.-Y. Chou, J. I. Dadap, F. Xia, W. M. J. Green, L. Sekaric, Y. A. Vlasov, R. M. Osgood, and K. Bergman, "Ultrahigh-bandwidth silicon photonic nanowire waveguides for on-chip networks," IEEE Photon. Technol. Lett. **20**, 398–400 (2008).
25. J. D. B. Bradley, M. C. Silva, M. Gay, L. Bramerie, A. Driessen, K. Wörhoff, J.-C. Simon, and M. Pollnau, "170 Gbit/s transmission in an erbium-doped waveguide amplifier on silicon," Opt. Express **17**, 22201–22208 (2009).

26. P. J. Winzer, G. Raybon, H. Song, A. Adamiecki, S. Corteselli, A. H. Gnauck, D. A. Fishman, C. R. Doerr, S. Chandrasekhar, L. L. Buhl, T. J. Xia, G. Wellbrock, W. Lee, B. Basch, T. Kawanishi, K. Higuma, and Y. Painchaud, "100-Gb/s DQPSK transmission: from laboratory experiments to field trials," J. Lightwave Technol. **26**, 3388–3402 (2008).
27. C. Gui, C. Li, Q. Yang, and J. Wang, "Demonstration of terabit-scale data transmission in silicon vertical slot waveguides," Opt. Express **23**, 9736–9745 (2015).
28. F. Horlin, J. Fickers, P. Emplit, A. Bourdoux, and J. Louveaux, "Dual-polarization OFDM-OQAM for communications over optical fibers with coherent detection," Opt. Express **21**, 6409–6421 (2013).
29. Z. Li, T. Jiang, H. Li, X. Zhang, C. Li, C. Li, R. Hu, M. Luo, X. Zhang, X. Xiao, Q. Yang, and S. Yu, "Experimental demonstration of 110-Gb/s unsynchronized band-multiplexed superchannel coherent optical OFDM/OQAM system," Opt. Express **21**, 21924–21931 (2013).